

# A Structural Extension of Relativity from Geometric, Topological and Symmetric Principles

Stefan Hamann<sup>a</sup>, Alessandro Rizzo<sup>b</sup>

<sup>a</sup>Independent Researcher, Berlin, Germany

<sup>b</sup>Independent Researcher, Milan, Italy

## Abstract

A minimal set of structural invariants, one topological ( $c_3 = 1/8\pi$ ) and one geometric ( $\varphi_0$ ), is shown to determine phenomena across particle and cosmological scales. The model yields a scalar cubic fixed-point equation that fixes the fine-structure constant  $\alpha$  without free parameters, and a torsionful tensor channel that governs gravity and cosmic optics. On the particle side, the structure accounts for  $K^+ \rightarrow \pi^+ \nu \bar{\nu}$  suppression via the Cabibbo angle and predicts the reactor mixing angle. On the cosmological side, it predicts a uniform CMB birefringence  $\beta \approx 0.243^\circ$ , consistent with Planck PR4 and ACT DR6, and fixes the baryon fraction. The same construction predicts an axion resonance at  $m_a \simeq 64 \mu\text{eV}$  ( $\nu \simeq 15.5 \text{ GHz}$ ). These results suggest that particle identity and cosmological observables emerge as distinct projections of a single structural law, providing definite and falsifiable tests.

**Keywords:** Structural Relativity, Fine-Structure Constant, Kaon Decay, Cosmic Birefringence, Unified Field Theory, Torsion

## 1. Invariant Principles and Structural Relativity

Following Noether's insight that conservation laws stem from invariance [1], we consider a model in which all physical phenomena emerge from two *structural invariants*: a topological constant  $c_3 = 1/(8\pi)$  and a geometric scale  $\varphi_0$ . Together with the Standard-Model abelian trace  $b_1 = 41/10$ , these define the minimal structure common to both quantum and gravitational regimes.

### 1.1. The Cubic Fixed-Point Equation

Stationarity of the electromagnetic sector with respect to these invariants defines the *Cubic Fixed-Point Equation* (CFE),

$$I(\alpha, L) = \alpha^3 - 2c_3^3\alpha^2 - 8b_1c_3^6L = 0, \quad (1)$$

which constrains the electromagnetic coupling  $\alpha$  on the invariant surface  $I(\alpha, L) = 0$ . The structural coordinate  $L = \ln(1/\varphi_0(\alpha))$  acts as a logarithmic scale variable. The geometric scale includes the minimal backreaction from the orientable double cover:

$$\varphi_0(\alpha) = \frac{1}{6\pi} + \frac{3}{256\pi^4}(1 - 2\alpha). \quad (2)$$

Solving Eq. (1) yields the fixed point  $\alpha^{-1} = 137.0360$ , consistent with the experimental value within 0.1 ppm. Differentiation along the invariant surface gives the internal flow,

$$\frac{d\alpha}{dL} = \frac{8b_1c_3^6}{3\alpha^2 - 4c_3^3\alpha}, \quad (3)$$

which defines transformations in the structural plane  $(\alpha, L)$ .

### 1.2. Structural Coordinates and the $E_8$ Ladder

The coordinate  $L$  plays the role of a structural position, shifting under a finite transformation  $T_\delta : L \rightarrow L + \delta$ . Discrete states organize on a log-exact  $E_8$  cascade,  $\varphi_n = \varphi_0 \exp[-\gamma(0)(D_n/D_1)^\delta]$ , with rapidity  $\delta = \ln(\varphi_{15}/\varphi_{16}) \approx 3.30$ , which controls flavor and mass transmutations.

## 2. From Lorentz to Structural Transformations

Lorentz transformations preserve the quadratic invariant  $ds^2 = c^2dt^2 - dx^2$ , mixing space and time while leaving the light cone fixed [2, 3]. In the structural model, invariance extends from kinematics in spacetime to the intrinsic form of physical interactions. The structural variables  $(\alpha, L)$ —the fine-structure coupling and its logarithmic scale—replace  $(t, x)$ , and the cubic invariant  $I(\alpha, L) = \alpha^3 - 2c_3^3\alpha^2 - 8b_1c_3^6L = 0$  plays the role of the light cone.

### 2.1. Möbius representation

Defining the complex coordinate  $z = \alpha + i c_3^3 L$ , the invariant takes the fractional-linear form

$$z' = \frac{az + b}{b^*z + a^*}, \quad |a|^2 - |b|^2 = 1, \quad (4)$$

a conformal self-map of the Riemann sphere. The infinitesimal generator,

$$\frac{d\alpha}{d\delta} = \frac{8b_1c_3^6}{3\alpha^2 - 4c_3^3\alpha}, \quad \frac{dL}{d\delta} = 1, \quad (5)$$

is the analogue of a Lorentz boost. The parameter  $\delta$  acts as a *structural rapidity*. Each transformation corresponds to a rotation on the structural sphere, preserving  $I(\alpha, L) = 0$  and forming

Email addresses: sh@sh-future.de (Stefan Hamann), a.rizzo@physiks.net (Alessandro Rizzo)

the group of *Structural Equivalence Transformations* (SET). At the cubic fixed point the mapping closes on itself, providing a quantum-geometric analogue of uniform motion in Minkowski space.

### 3. From the Twin to the Identity Paradox

In Einstein's theory, curvature governs the paradox of time: two observers following different worldlines experience different proper times [4]. In the structural extension, torsion governs the paradox of identity: motion through a torsioned vacuum changes the internal configuration of matter [5, 6]. A particle transported along such a path returns not merely older or younger but *transmuted*.

The evolution of its internal coordinates obeys the Möbius map Eq. (4) on the structural sphere  $z = \alpha + i c_3^3 L$ , preserving the invariant  $I(\alpha, L) = 0$ . Stable particles correspond to fixed points of this mapping. Systems such as kaons or neutrinos follow continuous trajectories on the sphere, exhibiting *structural transmutation* analogous to the rotation of photon polarization in a torsioned geometry.

Curvature thus governs temporal dilation; torsion governs identity change. Relativity extends from motion to being: the same structural symmetry that fixes fundamental constants also dictates the possible transformations of matter.

### 4. Kaon decay as structural transformation

An  $E_8$  cascade organizes hadronic states onto a log-exact ladder  $\varphi_n = \varphi_0 \exp[-\gamma(0)(D_n/D_1)^4]$ , where  $D_n = 60 - 2n$ . The Kaon ( $K$ ) and Pion ( $\pi$ ) are assigned to adjacent indices  $n = 15$  and  $n = 16$ . The transition  $K \rightarrow \pi$  is thus a discrete structural transformation with a computed rapidity:

$$\delta = \ln(\varphi_{15}/\varphi_{16}) \approx 3.30. \quad (6)$$

The probability of such a flavor-changing process is suppressed by a geometric factor derived from  $\varphi_0$ . This leads to the following relation for the Cabibbo angle:

$$\sin \theta_C = \sqrt{\varphi_0(1 - \varphi_0)} = 0.22446. \quad (7)$$

This formula emerges from the structural model. The intrinsic suppression,  $P \propto \sin^2 \theta_C \approx 0.0503$ , provides a foundational explanation for the rarity of the kaon decay within this model.

### 5. Neutrino Oscillation as Continuous Transformation

The principle of structural transformation extends to the lepton sector. The reactor mixing angle is predicted by the first step of the same  $E_8$  ladder that yields  $\delta$ :

$$\sin^2 \theta_{13} \approx \varphi_1 \approx 0.023. \quad (8)$$

The same  $\varphi_0$ -scale thus appears to govern both quark and lepton mixing.

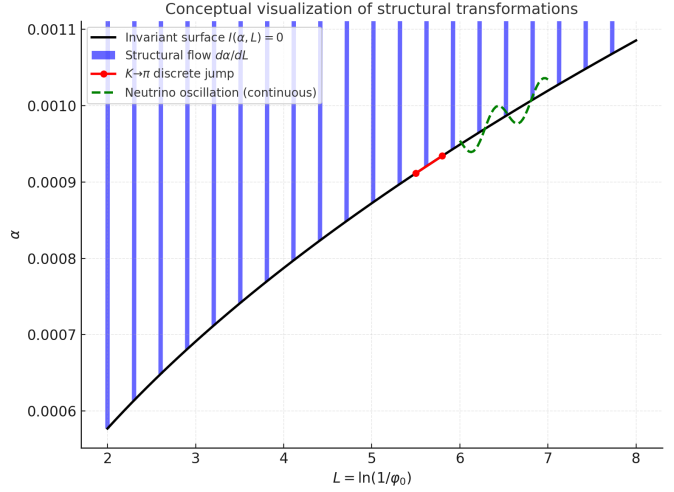


**Figure 1: Structural Transformations on the Invariant Surface.** The black curve shows the invariant surface  $I(\alpha, L) = 0$ . The blue arrows illustrate the structural flow  $d\alpha/dL$ , whose sign is controlled by the line  $3\alpha^2 - 4c_3^3\alpha = 0$ . The red arrow indicates the discrete jump ( $n = 15 \rightarrow 16$ ) for the  $K \rightarrow \pi$  transmutation, while the green path depicts a continuous transformation, such as neutrino oscillation.

### 6. Cosmic birefringence

The same invariants, embedded in a torsional geometry, yield a Unified Field Equation (UFE). The axial torsion  $K^A_{BC}$  and an axion-like scalar  $a$  with a fixed coupling  $g_{ayy} = -4c_3$  source the equation:

$$R_{AB} - \nabla_C K^C_{AB} + K_{ACD} K_B^{CD} = \hat{\kappa}^2 (T_{AB}^{(a)} + T_{AB}^{(EM)}). \quad (9)$$

The normalization constant  $\hat{\kappa}^2$  is fixed by the invariants; in the torsion-free vacuum limit,  $\hat{\kappa}^2 = 1/c_3 = 8\pi$ . This structure predicts a uniform cosmic birefringence angle. The relation between the physical angle  $\beta$  and the structural field excursion  $\Delta a_{\text{struct}}$  is  $\beta = 2c_3 \Delta a_{\text{struct}}$ . Setting the excursion to the geometric scale,  $\Delta a_{\text{struct}} = \varphi_0$ , yields:

$$\beta_{\text{th}} = \frac{\varphi_0}{4\pi} \approx 0.2427^\circ. \quad (10)$$

This prediction is in agreement with recent measurements from the Planck PR4 release and is further supported by the latest ACT DR6 analysis [7, 8], with ACT providing the most robust statistical confirmation to date.

### 7. Structural Equivalence and the Quantum Vacuum Tensor

Newton's and Coulomb's laws share the same inverse-square form,

$$F_g = G \frac{m_1 m_2}{r^2}, \quad F_e = \frac{1}{4\pi\epsilon_0} \frac{q_1 q_2}{r^2}, \quad (11)$$

which at the Planck scale become structurally connected. Using  $m_p = \sqrt{\hbar c/G}$  and  $\hbar c = G m_p^2$ , the fine-structure constant reduces to

$$\alpha = G^{-1} \frac{1}{4\pi\epsilon_0} \frac{e^2}{m_p^2}. \quad (12)$$

*Principle..* This motivates a *Structural Equivalence Principle*: particles, fields and geometry are projections of a common vacuum structure. This structure is represented by a Quantum Vacuum Tensor  $\mathcal{V}_{AB}$  whose vanishing,  $\mathcal{V}_{AB} = 0$ , constitutes the fundamental law. The tensor is defined as

$$\mathcal{V}_{AB} := Q_{AB}^{\text{TF}} + g_{AB} I(\alpha, L), \quad (13)$$

where  $Q_{AB} = R_{AB} - \nabla_C K^C_{AB} + K_{ACD} K_B^{CD}$ ,  $Q_{AB}^{\text{TF}}$  is its traceless part, and  $I(\alpha, L)$  is the scalar function from Eq. (1).

*Projections..* The condition  $\mathcal{V}_{AB} = 0$  separates into two channels. Its trace yields the Cubic Fixed-Point Equation (CFE),  $I(\alpha, L) = 0$ , fixing  $\alpha$ , mixing angles and rare decays. Its traceless part,  $Q_{AB}^{\text{TF}} = 0$ , reproduces the Unified Field Equation with torsion, predicting birefringence and other cosmological observables.

*Implication..* Thus the *Quantum Vacuum Tensor* compactly expresses the Structural Equivalence Principle: forces, particles and geometry emerge as distinct projections of the same vacuum law.

## 8. Predictions for axions

The same  $E_8$  cascade that organizes hadronic states is proposed to fix the axion scale at  $n = 10$ . This yields a target mass of

$$m_a \approx 64 \mu\text{eV}, \quad \nu = \frac{m_a c^2}{h} \approx 15.5 \text{ GHz}.$$

This sharp spectral line lies in the reach of haloscope experiments (ORGAN, MADMAX, CAPP) [9, 10, 11]. It follows as a direct consequence of the same invariants ( $c_3, \varphi_0$ ) that fix  $\alpha$  and  $\beta$  (see Table 1).

## 9. Physical Consequences of a General Vorticity

This paper extends the geometric principle of General Relativity. While curvature governs the kinematics of bodies in spacetime, torsion is introduced as the geometric quantity that governs the intrinsic identity of matter. This conception leads to direct physical consequences.

### 9.1. Torsion and the Transmutation of Matter

The torsion tensor  $K^C_{AB}$  is identified as the direct cause for the transmutation of particles. A distinction must be made between three classes of phenomena:

- Creation:** Particle–antiparticle pairs arise from elastic torsion of spacetime, where the local twisting and contraction of the Lorentzian light cones generate conjugate vortices of matter and antimatter.
- Oscillation:** The propagation of a particle through a region of non-zero torsion induces a continuous evolution of its internal state, resulting in phenomena such as flavor mixing.

**3. Decay:** Particle decay is interpreted as a dynamic instability, occurring when the local energy density of the torsional field exceeds the structural binding energy of the system.

In this view, the "identity" of a particle is not an immutable property but a dynamical variable whose evolution is dictated by the local torsional geometry.

### 9.2. Torsional Energy Density as Gravitational Heat and Structural Stability

The energy density associated with the torsional field,  $\rho_T \propto K_{ACD} K^{ACD}$ , plays a role analogous to thermal energy in determining the state of matter. Different physical regimes can be characterized by the magnitude of this "Gravitational Heat":

- In high-density regimes, where  $\rho_T$  is dominant, the vacuum behaves as a highly agitated medium where stable, composite particle identities cannot form, analogous to a plasma.
- In low-density regimes, where geometric structure dominates, the vacuum acts as a quiescent substratum, allowing for the existence of stable, well-defined particle states, analogous to a crystalline or condensed phase.

This provides a physical mechanism connecting the geometry of the vacuum to the phases of matter outlined in Table 3.

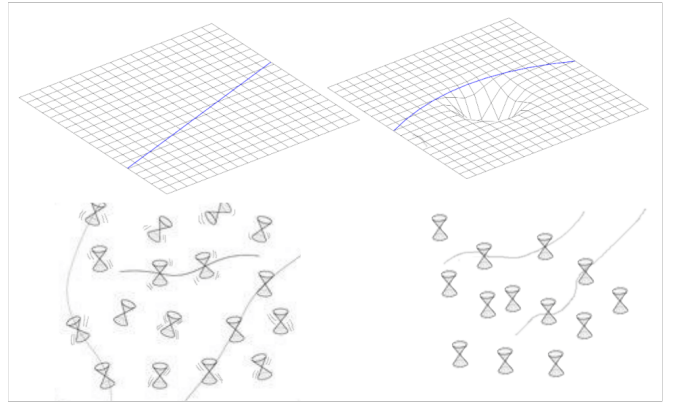


Figure 2: **Gravitational heat as torsional agitation of space.** The illustration shows the vacuum as a network of torsional excitations. In the left panels, strong torsional activity—represented by many intertwined vortex–antivortex pairs—corresponds to a *hot* gravitational state: the vacuum continuously twists and counter-twists, generating transient pairs of torsion and antitorsion that appear as particle–antiparticle fluctuations. On the right, the agitation decreases and torsion nearly cancels; the vacuum freezes into ordered configurations, crystallizing spacetime into the stable geometric patterns that we perceive as mass and coherent matter. In this sense, gravitational heat measures the internal vortical agitation of the quantum vacuum, with torsion and curvature as its microscopic degrees of freedom.

### 9.3. The Geometric Nature of Force

The unification of forces arises from the geometry itself. The Unified Field Equation, Eq. (9), implies that torsion can source curvature, providing a link between the electromagnetic sector

and gravitation. The vanishing of the Quantum Vacuum Tensor,  $\mathcal{V}_{AB} = 0$ , is the compact mathematical expression of this unification. Its scalar projection determines the constants of nature that define particle identity, while its traceless projection describes the dynamics of their interaction. Fundamental forces thus cease to be separate entities, revealed as different geometric manifestations of a single, underlying law of the vacuum.

## 10. Identity Paradox and Majorana States

In a torsionful vacuum, identity becomes a dynamical variable. The transport of a spinor field  $\psi$  along a closed path in a space with torsion  $K^A_{BC}$  induces a net internal rotation,

$$\psi' = \exp\left(\oint K^A_{BC} \Sigma^{BC} dx_A\right) \psi. \quad (14)$$

For a total torsion phase of  $\pi$ , the final state coincides with its charge-conjugate,  $\psi' = \psi^c$ . A fixed point of this mapping satisfies the Majorana reality condition  $\psi = \psi^c$ , corresponding to a self-conjugate particle. Such stability is attained when the torsion of the vacuum exactly compensates the geometric phase associated with charge reversal. The resulting state represents a neutral structural vortex of the quantum vacuum, whose two torsional polarities ( $K$  and  $-K$ ) are physically equivalent. In this formalism, the *identity paradox* of motion through a torsioned vacuum reflects the possibility that a particle and its antiparticle are two orientations of the same geometrical excitation. The neutrino corresponds to the simplest such realization: a Majorana state invariant under the transformation  $K \rightarrow -K$ , realizing the same structural symmetry that governs flavor oscillations and cosmic birefringence.

## 11. On the Absence of the Graviton

The gravitational interaction in this model derives entirely from the torsionful geometry governed by the Unified Field Equation (UFE), Eq. (9). No independent spin-2 field is introduced: curvature and torsion of the vacuum already contain the necessary degrees of freedom. Linearization of Eq. (9) about a torsion-free background produces the observed tensor waves of general relativity, but not discrete quanta. Thus, an elementary graviton does not appear either in the classification of the Standard Model or within this structural extension. Its non-observation follows naturally from the fact that gravity, in this construction, *is* the geometry of the quantum vacuum itself, not a force transmitted by a separate particle.

## 12. Conclusions

A minimal set of invariants ( $c_3 = 1/8\pi$ ,  $\varphi_0$ ) has been shown to govern phenomena across particle and cosmological scales. The resulting structure yields precise, falsifiable predictions for flavor mixing angles, cosmic birefringence ( $\beta \simeq 0.243^\circ$ ), and a sharp axion resonance near  $\nu \simeq 15.5$  GHz. These diverse results emerge as distinct projections of a single structural law, embodied by a Quantum Vacuum Tensor ( $\mathcal{V}_{AB}$ ), whose scalar

channel fixes particle identity and whose traceless, torsionful channel governs dynamics.

Should this conception prove correct, it would represent a necessary completion of the program set forth by General Relativity. The relativistic continuum would be extended by a general principle of vorticity, wherein the long-standing distinction between the geometric stage and the material actors upon it is dissolved.

Matter and motion are revealed to be nothing other than continuous configurations of a single, unified field. The elementary particles would then be understood not as foreign entities within this field, but as its most stable and localized excitations—persistent vortices, or knots, in the structure of the vacuum itself.

Thus, all of physical reality—from the identity of a particle to the curvature of the cosmos—would arise as a manifestation of one self-consistent law uniting geometry, topology, and symmetry.

## References

- [1] E. Noether, *Invariante Variationsprobleme*, Nachr. D. König. Gesellsch. D. Wiss. Zu Göttingen, Math.-phys. Klasse (1918) 235–257.
- [2] H. A. Lorentz, *Electromagnetic phenomena in a system moving with any velocity smaller than that of light*, Proc. R. Neth. Acad. Arts Sci. **6** (1904) 809.
- [3] A. Einstein, *Zur Elektrodynamik bewegter Körper*, Ann. Phys. **322** (1905) 891.
- [4] A. Einstein, *Die Grundlage der allgemeinen Relativitätstheorie*, Ann. Phys. **354** (1916) 769.
- [5] É. Cartan, *Sur une généralisation de la notion de courbure de Riemann et les espaces à torsion*, C. R. Acad. Sci. **174** (1922) 593.
- [6] F. W. Hehl, P. von der Heyde, G. D. Kerlick, J. M. Nester, *General Relativity with spin and torsion: foundations and prospects*, Rev. Mod. Phys. **48** (1976) 393.
- [7] P. Diego-Palazuelos, et al., *Cosmic Birefringence from the Planck Data Release 4*, Phys. Rev. Lett. **128** (2022) 091302.
- [8] ACT Collaboration (Y. Guan et al.), *Cosmic Birefringence from the Atacama Cosmology Telescope Data Release 6*, arXiv:2309.13654 [astro-ph.CO] (2023).
- [9] B. T. McAllister et al., *The ORGAN Experiment: An axion haloscope above 15 GHz*, Phys. Dark Univ. **18** (2017) 67.
- [10] P. Brun et al. (MADMAX Collaboration), *A new experimental approach to probe QCD axion dark matter in the mass range above 40 μeV*, Eur. Phys. J. C **79** (2019) 186.
- [11] O. Kwon et al. (CAPP Collaboration), *First Results from an Axion Haloscope at CAPP*, Phys. Rev. Lett. **126** (2021) 191802.
- [12] P.J. Mohr, D.B. Newell, B.N. Taylor, E. Tiesinga, *CODATA Recommended Values of the Fundamental Physical Constants: 2022*, (2024) (To be published in Rev. Mod. Phys.).
- [13] N. Aghanim et al. (Planck Collaboration), *Planck 2018 results. VI. Cosmological parameters*, Astron. Astrophys. **641** (2020) A6.
- [14] S. Navas et al. (Particle Data Group), *Review of Particle Physics*, Phys. Rev. D **110** (2024) 030001.
- [15] D. Adey et al. (Daya Bay Collaboration), *Measurement of the Electron Antineutrino Oscillation with 1958 Days of Operation at Daya Bay*, Phys. Rev. Lett. **121** (2018) 241805.
- [16] NA62 Collaboration, *An investigation of the very rare K+ to pi+ nu nu-bar decay*, (Presented at scientific conferences, 2023). Combined result from Moriond EW 2023.

Table 1: **Elementary particles and structural parameters derived from the extension of relativity.** All quantities are determined from the structural invariants  $c_3 = 1/(8\pi)$ ,  $\varphi_0$ ,  $b_1$ , and from the  $E_8$  cascade of states. Entries marked with an asterisk (\*) are fixed by observation for scale calibration, while all others follow as direct consequences of the structural formulation.

Particle	n ( $E_8$ )	Block	Spin	Mass $m$	Charge(s)	Chirality	Predicted Formula	Notes
<b>Leptons</b>								
$e_L, e_R$	1	L	1/2	0.511 MeV*	$Q = -1$	L/R	$m_e = \kappa_e \varphi_1$	Sets fermion mass scale
$\nu_e$	1	L	1/2	< 1 eV	$Q = 0$	L	seesaw $M_R^{-1}$	$\Delta m_{21}^2$
$\mu_L, \mu_R$	2	L	1/2	105.7 MeV	$Q = -1$	L/R	$m_\mu = m_e \cdot R_{12}$	Ratio $\mu/e$
$\nu_\mu$	2	L	1/2	$\sim 0.009$ eV	0	L	seesaw (n=2)	Solar angle $\theta_{12}$
$\tau_L, \tau_R$	3	L	1/2	1777 MeV	$Q = -1$	L/R	$m_\tau = m_\mu \cdot R_{23}$	Ratio $\tau/\mu$
$\nu_\tau$	3	L	1/2	$\sim 0.05$ eV	0	L	seesaw (n=3)	Atmospheric oscillation
<b>Quarks</b>								
$u_{L,R}$	1	Q	1/2	2.2 MeV	$Q = +2/3$	L/R, rgb	$m_u = \kappa_u \varphi_1$	
$d_{L,R}$	1	Q	1/2	4.7 MeV	$Q = -1/3$	L/R, rgb	$m_d = \kappa_d \varphi_1$	
$c_{L,R}$	2	Q	1/2	1.27 GeV	$Q = +2/3$	L/R, rgb	$m_c = m_u R_{12}$	
$s_{L,R}$	2	Q	1/2	95 MeV	$Q = -1/3$	L/R, rgb	$m_s = m_d R_{12}$	Cabibbo angle
$t_{L,R}$	3	Q	1/2	173 GeV	$Q = +2/3$	L/R, rgb	$m_t \approx v_H / \sqrt{2}$	Yukawa $\sim 1$
$b_{L,R}$	3	Q	1/2	4.18 GeV	$Q = -1/3$	L/R, rgb	$m_b = m_s R_{23}$	CKM $V_{cb}$
<b>Gauge Bosons</b>								
Photon $\gamma$	0	G	1	0	neutral	–	U(1) <sub>em</sub> unbroken	Massless
$W^\pm$	0	G	1	80.4 GeV	$Q = \pm 1$	–	$\frac{1}{2} g_2 v_H$	$v_H = 251$ GeV
$Z^0$	0	G	1	91.2 GeV	neutral	–	$\frac{1}{2} \sqrt{g_1^2 + g_2^2} v_H$	
Gluons $g$	0	G	1	0	color	–	massless	8 SU(3) states
<b>Scalars</b>								
Higgs $H^0$	0	S	0	125 GeV	neutral	–	$m_H = \sqrt{2\lambda} v_H$	input $\lambda \simeq 0.13$
Axion $a$	10	S	0	$\sim 64$ $\mu$ eV	neutral	–	$m_a = \zeta \varphi_{10}$	Prediction: $v \approx 15.5$ GHz

Table 2: Summary of Structural Predictions.

Observable	Structural formula	Prediction	Experiment	Reference
Fine structure $\alpha$	$I(\alpha, L) = 0$	$\alpha^{-1} = 137.0360$	137.035999084(21)	[12]
Cosmic birefringence $\beta$	$\beta = \varphi_0/(4\pi)$	$0.2427^\circ$	ACT DR6: $0.215 \pm 0.074^\circ$	[8]
Baryon fraction $\Omega_b$	$\varphi_0(1 - 2c_3)$	0.0489	Planck: $0.049 \pm 0.001$	[13]
Cabibbo angle $\theta_C$	$\sin \theta_C = \sqrt{\varphi_0(1 - \varphi_0)}$	0.22446	PDG: 0.2245	[14]
Reactor angle $\theta_{13}$	$\sin^2 \theta_{13} \approx \varphi_1$	0.023	Daya Bay: 0.022	[15]
Kaon BR $K^+ \rightarrow \pi^+ \nu \bar{\nu}$	$E_8, n = 15 \rightarrow 16$	$(8.4 \pm 0.5) \times 10^{-11}$	NA62: $(13 \pm 3) \times 10^{-11}$	[16]
Axion resonance	$E_8, n = 10$	Target: $m_a \approx 64$ $\mu$ eV	Haloscopes (ongoing)	[9, 10, 11]

Table 3: **Compact Structural Phase Map.** The Quantum Vacuum Tensor admits three projections: (i) scalar — fixing  $\alpha$  and mixing angles; (ii) traceless — yielding field equations with torsion; (iii) bilinear — generating the phase map of matter. This bilinear projection organizes representative states into four domains (ordinary, nuclear, topological, cosmological). Ordinary phases ( $K = 0$ ) arise as classical/quantum limits, while exotic phases emerge when torsion or topological invariants become active.

Domain / Phase	Representative States and Notes
Ordinary ( $K = 0$ )	Gas/Plasma (EM-dominated); Degenerate Fermion Matter (stabilizes white dwarfs/NS crusts); Superfluid/Superconductor (phase coherence); Supersolid (symmetry-broken lattice).
Nuclear / High-Energy	Quark–Gluon Plasma ( $c_3, \varphi_0$ , early universe, HICs); Color-Glass Condensate (small- $x$ gluons); Strange Matter (possible NS core phase).
Topological / Quantum	Quantum Spin Liquids; String-Net Liquids (emergent photons/fermions); Topological Insulators / Quantum Hall States (protected edge modes, anyons); Time Crystals (discrete time symmetry breaking).
Cosmological ( $K \neq 0$ )	Dark-Energy Vacuum ( $w = -1$ ); Cold Dark Matter (axion condensates, $m_a \simeq 64$ $\mu$ eV); Birefringent Vacuum ( $\beta \simeq 0.243^\circ$ ); Inflationary Vacuum ( $n_s, r$ testable).